Antibacterial and bioactive silver-containing $Na_2O \cdot CaO \cdot 2SiO_2$ glass prepared by sol–gel method

M. CATAURO, M. G. RAUCCI, F. DE GAETANO, A. MAROTTA
Department of Materials and Production Engineering, University of Naples "Federico II", Piazzale Tecchio 80, 80125 Naples, Italy
E-mail: catauro@unina.it

The antibacterial effect of addition of silver oxide to $Na_2O \cdot CaO \cdot 2SiO_2$ glass have been studied. Silver containing and silver free $Na_2O \cdot CaO \cdot 2SiO_2$ glasses have been prepared by sol–gel synthesis using tetramethil orthosilicate, sodium ethoxide, calcium nitrate tetrahydrate and silver nitrate as starting materials and methyl ethyl ketone as solvent. The gel was examined by differential thermal analysis, thermo gravimetric analysis, FTIR spectroscopy and X-ray diffraction analysis. Antibacterial and bioactive tests on gel glass powders, obtained after a heat treatment of 2 h at 600 °C of the dried gel, were carried out. High antimicrobial effects of samples against *Escherichia coli* and *Streptococcus mutans* were found. FTIR measurements and SEM micrographs have ascertained the formation of a hydroxyapatite layer on the surface of samples soaked in a simulated body fluid for different times.

1. Introduction

Antimicrobial ceramics are becoming increasingly important because of their wide range of applications, including fabrics, building materials, cosmetics, electrical appliances, etc. It is known that certain metal ions penetrate into bacteria and inactivate their enzymes or some metal ions can generate hydrogen peroxide, thus killing bacteria [1]. Several metal ions have been used in antimicrobial ceramics, such as Ag^+, Cu^{2+}, Zn^{2+}, etc. Recently, various inorganic antibacterial materials containing silver have been developed. Silica materials containing silver is expected to be candidate of such antibacterial material for various applications, since it is assumed to show high chemical durability. It is well known, in fact, that silica and calcium–silica gels have good bioactivity and biocompatibility *in vitro*, so they are used as implant biomaterials because they possess similar structure to the major mineral constituent of human hard bone [2–4].

There is much interest in silver containing glasses and ceramics for use in bone replacement [5–7] as well as wastewater treatment [8, 9] owing to the demonstrated antimicrobial effects.

The sol–gel derived silica glass powder containing silver with composition $Al/Ag \geq 1$ are believed to be useful as an antibacterial material for medical applications such as filler of composite resin for dental restoration.

In orthopaedic realm, silver-containing biomaterials with bone bonding properties would be especially desirable [10].

In the present study, silver containing silica material was prepared by sol–gel method, with the purpose to analyse its bioactivity and antibacterial properties. The bioactivity was investigated soaking this material in simulated body fluid (SBF) at 37 °C to study the surface hydroxyapatite (HA) formation. The antimicrobial effects of gel against *Escherichia coli* and *Streptococcus mutans* (which is known as a major bacterium, inducing caries) were also examined.

2. Experimental

$Na_2O \cdot CaO \cdot 2SiO_2$ gel and $Na_2O \cdot CaO \cdot 2SiO_2$ gel containing 0.50 wt % Ag_2O were prepared by means of sol–gel method, using methyl ethyl ketone (MEK) as solvent, from analytical reagent grade sodium ethoxide, C_2H_5NaO, silver nitrate, $AgNO_3$, calcium nitrate tetrahydrate, $Ca(NO_3)_2 \cdot 4H_2O$ and tetramethyl orthosilicate (TMOS). Fig. 1 shows the flow chart of gel synthesis containing Ag_2O by sol–gel method. As can be seen, part of water was added together with the calcium nitrate. Water was also added later till a molar ratio to TMOS 4/1. After the gelation, the gels were dried in the open holder at 50 °C for five days.

Fourier transform infrared transmittance spectrum of dried gel was recorded in the 400–4000 cm^{-1} region, using a Nexus FTIR Thermo Nicolet. KBr pelletted disk containing 2 mg of sample and 200 mg of KBr was made.

The nature and the temperatures of the various reactions that occur during the heating of the dried gels were determined using differential thermal analysis

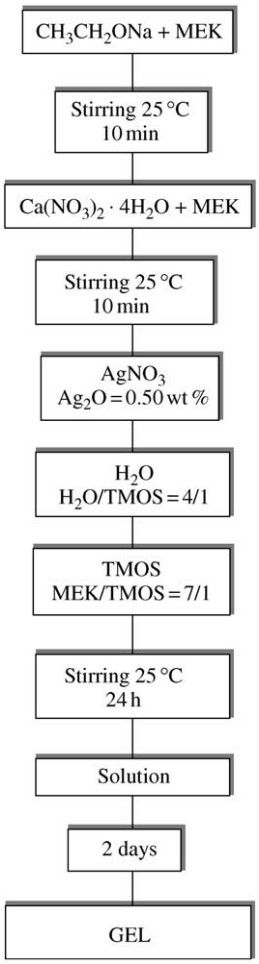

Figure 1 Flow chart of $Na_2O \cdot CaO \cdot 2SiO_2$ gel containing 0.50 wt % Ag_2O synthesis.

(DTA) and thermo gravimetric analysis (TGA). Powder samples (50 mg) of the dried gels were subjected to DTA and TGA runs at a heating rate of 10 °C/min from room temperature to 1200 °C. A Netsch DSC 404 and a Perkin Elmer TGA 7 equipped with high temperature furnaces were employed.

The amorphous or crystalline nature of gels glass powders were ascertained by X-ray diffraction (XRD), using a Philips diffractometer. Powders of sample were scanned from $2\Theta = 5$ to 60° using CuKα radiation.

The bacterium *E. coli* and the bacterium *S. mutans* (which is known as a major bacterium, inducing caries) were used in this study to test the antibacterial property of the gel glass.

Gel glass powders, with grains of diameter $90\,\mu m \leq d \leq 125\,\mu m$ were soaked in a SBF using a solid/solution ratio 0.25 g/50 ml, for different times, 7, 14 and 21 days, as it is prescribed for ''*in vitro*'' bioactivity tests by other researchers [11, 12, 15]. The ion concentrations of the SBF, reported in Table I, are nearly equal to those of the human blood plasma. The SBF was prepared by dissolving reagent grade NaCl, $NaHCO_3$, KCl, $MgCl_2$, HCl 1 M, $CaCl_2 \cdot 6H_2O$, Na_2SO_4, TRIS (trihydroxymethylaminomethane), and Na_2HPO_4. During soaking the temperature was kept at 37 °C.

The ability to form an apatite layer was tested using IR spectroscopy in the 400–1200 cm^{-1} region.

An electron microscope (SEM) (Cambridge Stereoscan 240) equipped with an energy dispersive analytical system (EDS) LINK AN 10000 was used in order to verify the morphology of the apatite deposition and to make a qualitative elemental analysis.

TABLE I Ion body concentration (mM) of simulated fluid and human blood plasma

Ion	Simulated body fluid	Blood plasma
Na^+	142.0	142.0
K^+	5.0	5.0
Mg^{2+}	1.5	1.5
Ca^{2+}	2.5	2.5
Cl^-	147.8	103.0
HCO_3^-	4.2	27.0
HPO_4^-	1.0	1.0
SO_4^{2-}	0.5	0.5

3. Results and discussion

3.1. Gel synthesis

The following reactions are responsible for gel formation [13]:

$$Si(OCH_3)_4 + nH_2O \Rightarrow Si(OCH_3)_{4-n}(OH)_n + nCH_3OH \quad \text{(hydrolysis)} \quad (1)$$

$$-SiOH + CH_3O\text{–}Si \Rightarrow -Si\text{–}O\text{–}Si- + CH_3OH \quad \text{(dealcoholation)} \quad (2)$$

$$-Si\text{–}OH + OH\text{–}Si- \Rightarrow -Si\text{–}O\text{–}Si- + H_2O \quad \text{(dehydration)} \quad (3)$$

$$Na(C_2H_5O) + -Si\text{–}OH \Rightarrow -Si\text{–}O^-\ Na^+ + C_2H_5OH \quad (4)$$

Mixing at low temperature allows the introduction of modifier cation, Na^+, into silicate network, according to Equation 4. The reaction mechanisms are not known in every detail, however, it is generally accepted that they proceed through a second-order nucleophilic substitution [14]. The interaction between the electrophilic metal and the nucleophilic agent (H_2O or $C_2H_5O^-$) gives rise to addition (Equation 1) or substitution (Equation 4) reactions, respectively. Sodium ethoxide works simultaneously as reagent and catalyst in substitution reactions.

Fig. 2 shows the infrared trasmission spectrum of dried gel. The bands at 3500 and 1620 cm^{-1} are attributed respectively to stretching and bending of O–H in water [13, 15, 16]. The 1385 cm^{-1} band is due to NO_3^- stretching modes [13]. The peak at 1067 cm^{-1} is due to the Si–O asymmetric stretching, at 950 cm^{-1} to Si–O non-bridging stretching, at 799 cm^{-1} to the Si–O symmetric stretching and at 447 cm^{-1} to the Si–O–Si bending [17, 18].

Fig. 3 shows the DTA curve of the as dried gel. A large endothermic peak, from room temperature to about 250 °C, and a simultaneous weight loss occurs in the TGA curve (Fig. 4). These effects were due to evaporation from open pore of the solvents physically trapped in the gel. A smaller endothermic effect occurs on DTA curve at about 450 °C that should be related to the pyrolisis of residual organic groups in the gel, which

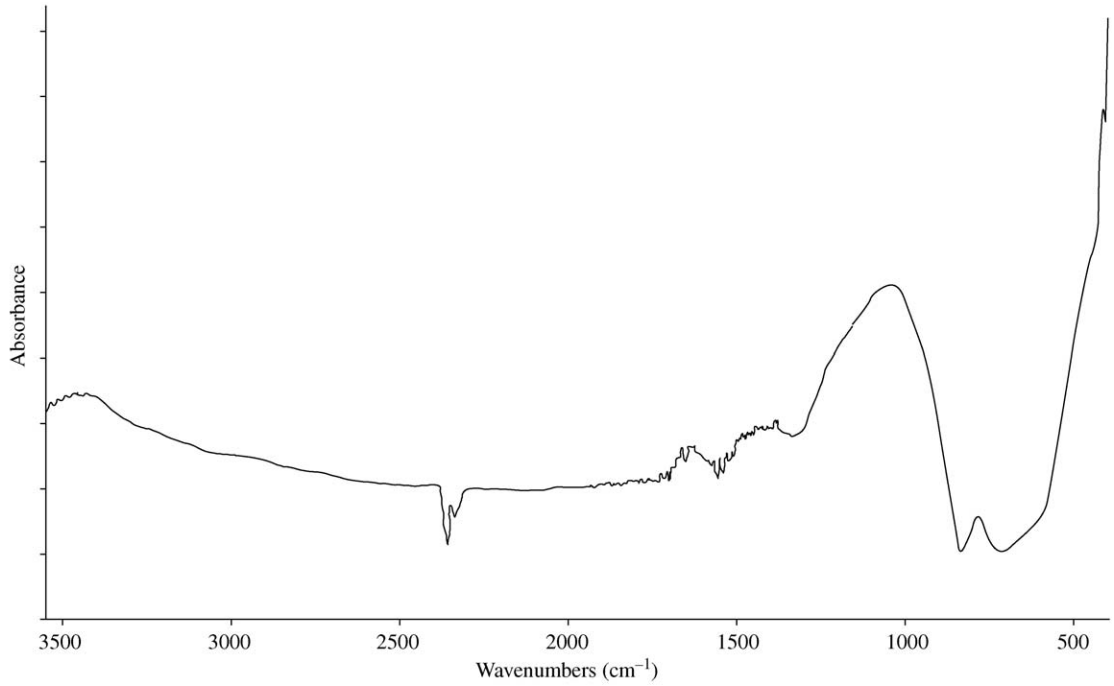

Figure 2 FTIR of the silver containing dried gel.

had not reacted by the end of the drying step and consequently did not evaporate from the gel before calcining. A simultaneous weight loss was detected on TGA curve in the same temperature range. At the end of the run a 35% of weight loss can be estimated.

The DTA of the gel exhibits also a slope change of the baseline at about 800 °C that may be attributed to the glass transition of the glass being formed, followed by a small exothermic peak at 887 °C due to a devitrification process. Finally an endothermic peak caused by the fusion of the crystallised phase occurs at 1042 °C.

To convert the gel into glass powders samples of the dried gel were held 2 h at 600 °C. The X-ray diffraction pattern, Fig. 5, of the gel glass powders after calcination at 600 °C exhibits broad humps characteristic of the amorphous nature of the samples. Antibacterial and bioactivity tests were carried out on samples of gel glass powders.

3.2. Antibacterial tests

Antibacterial property was examined by mixing 0.5 g of gel with glass powder with 5 ml of Tryptone Water Dehydrated physiologic solution. The same physiologic solution was used for bacteria. Five hundred microliter of containing bacteria solution were inoculated in 1 ml of sample solution. Sample and bacteria were in contact in plate at room temperature for 15, 30 min, 1 and 2 h. After each sampling time, EC X-GLUC agar for *E. coli* and AZIDE MALTOSE agar (KF) for *S. mutans* were added

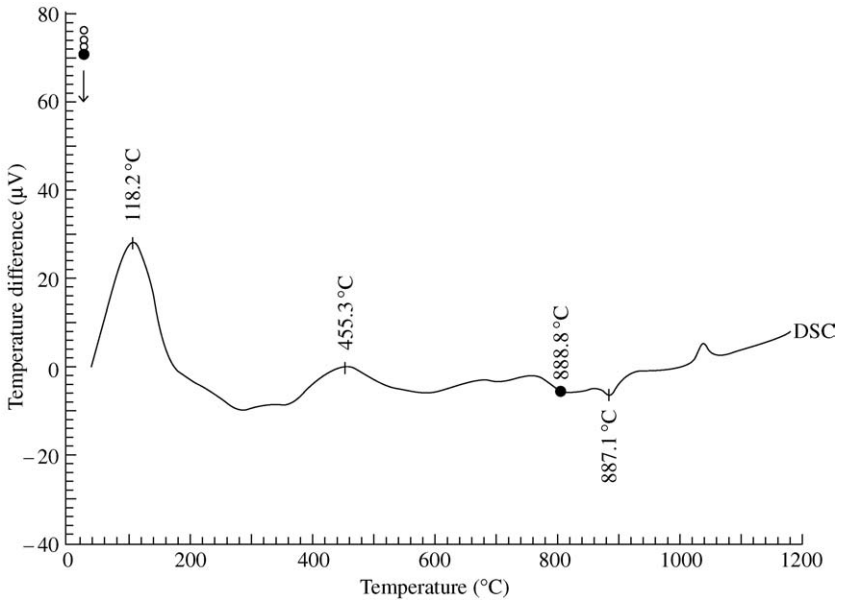

Figure 3 DTA curve of the silver containing dried gel.

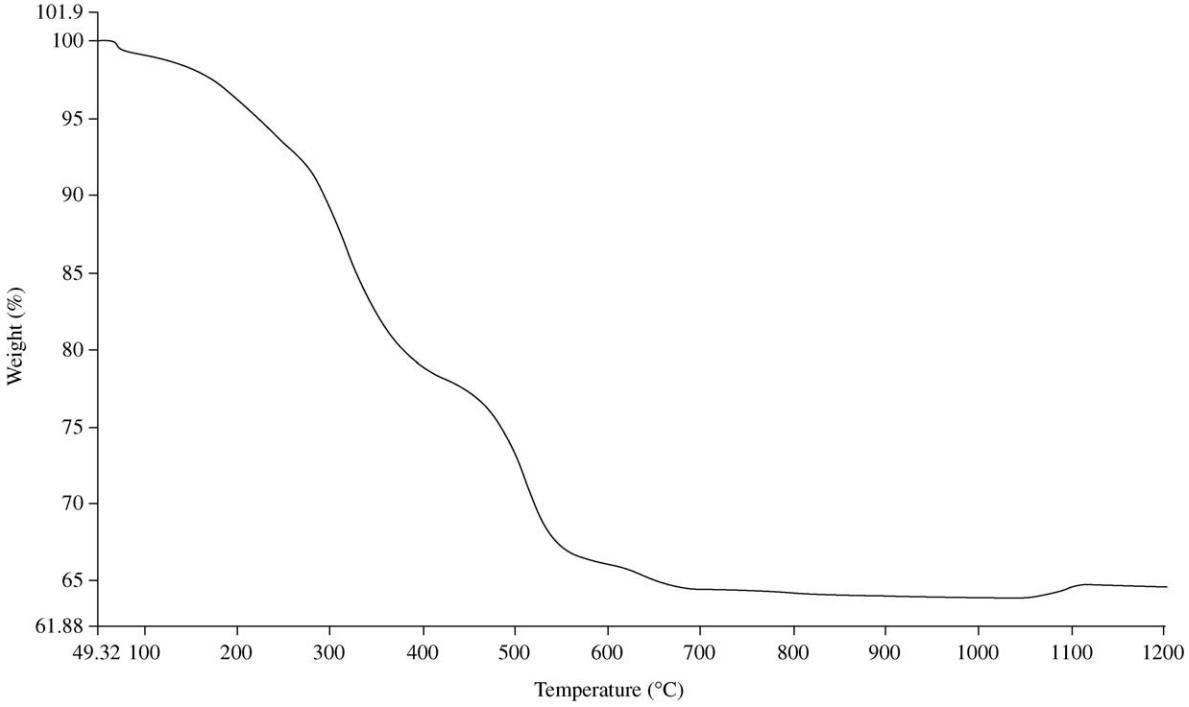

Figure 4 TGA curve of the silver containing dried gel.

to sample plates. The plates were aerobically incubated 24 h at 44 °C for *E. coli*, but anaerobically 48 h at 37 °C for *S. mutans*. The number of the colonies was counted. The comparison of cell-forming unit with a control with physiologic solution, bacteria and agar, without any foreign substances were made.

Antibacterial property was examined also for the gel not silver containing.

Table II shows the complete inhibition of the growth of *E. coli* after only 2 h of contact with the studied gel glass silver containing, and no inhibition was found for the silver free gel glass. The same results were observed with *S. mutans*.

These results indicate that the sample silver containing shows a high antibacterial activity against *E. coli* and *S. mutans* and are consistent with the antimicrobial effect of silver and silver containing materials [19].

3.3. Bioactivity tests

The FTIR spectra of silver containing and silver free samples after soaking in SBF for ''*in vitro*'' bioactivity tests are reported in Figs. 6 and 7. These spectra evidence the formation of an HA layer given by the appearance of the 1160 and 1035 cm^{-1} bands, usually assigned to the P–O stretching [18], and of the 610 cm^{-1} band, usually assigned to P–O bending mode [18]. The splitting after seven days soaking, of the 610 cm^{-1} band into two others at 640 and 600 cm^{-1} can be attributed to formation of crystalline HA [18]. Finally, the band at 800 cm^{-1} can be assigned to the Si–O–Si band vibration between two adjacent tetrahedra characteristic of silica gel [18]. This supports the hypothesis that a surface layer of silica gel forms as supposed in the mechanism proposed in the literature for hydroxyapatite deposition [12, 20].

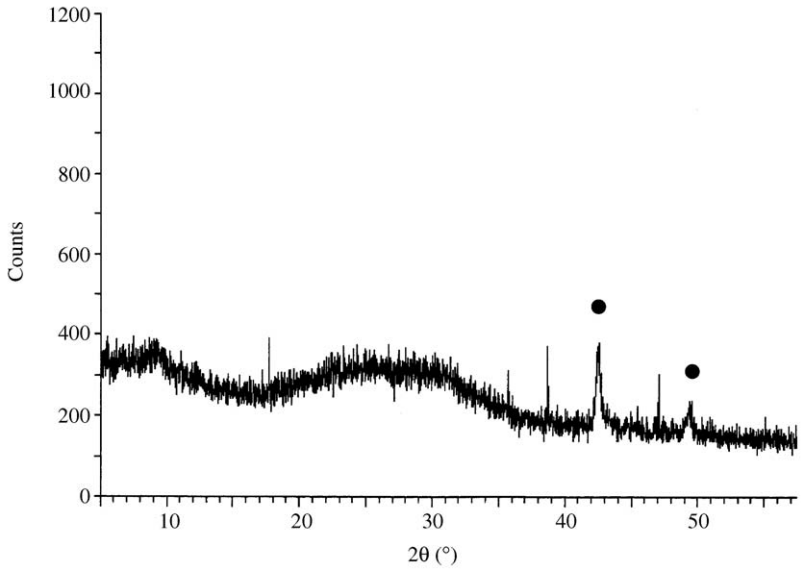

Figure 5 X-ray diffraction pattern shows amorphous nature of the silver containing gel glass after the calcinations 2 h at 600 °C, (•) holder.

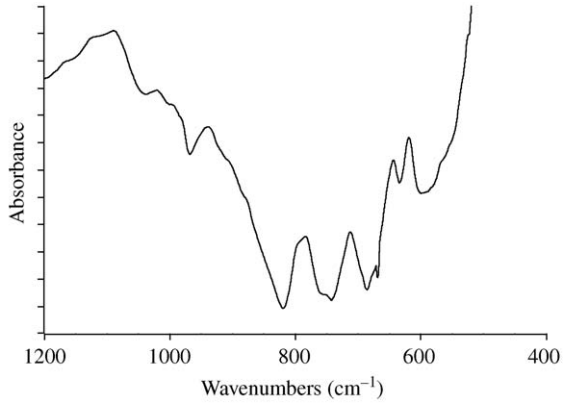

Figure 6 FTIR spectra of silver containing sample soaked 14 days in SBF.

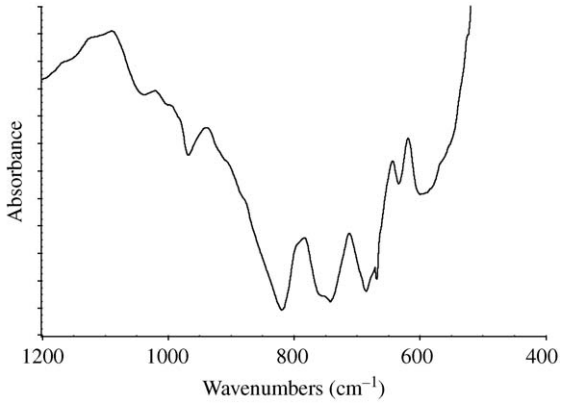

Figure 7 FTIR spectra of silver free containing sample soaked 14 days in SBF.

TABLE II Species bacteria

Incubation time (min)	*E. coli* (UFC)	*S. mutans* (UFC)
0	8000	1100
15	200	150
30	120	80
60	13	10
120	0	0

Moreover an evaluation of the morphology of the apatite deposition and a qualitative elemental analysis were carried out by electron microscopy observations.

In Figs. 8 and 9(a) the SEM micrograph of the same samples soaked in SBF for 14 days. The characteristic apatite globular crystals are clearly visible. As it can be seen, the EDS reported in Figs. 8 and 9(b) confirm that the surface layer observed in the SEM micrographs is composed of calcium and phosphorous.

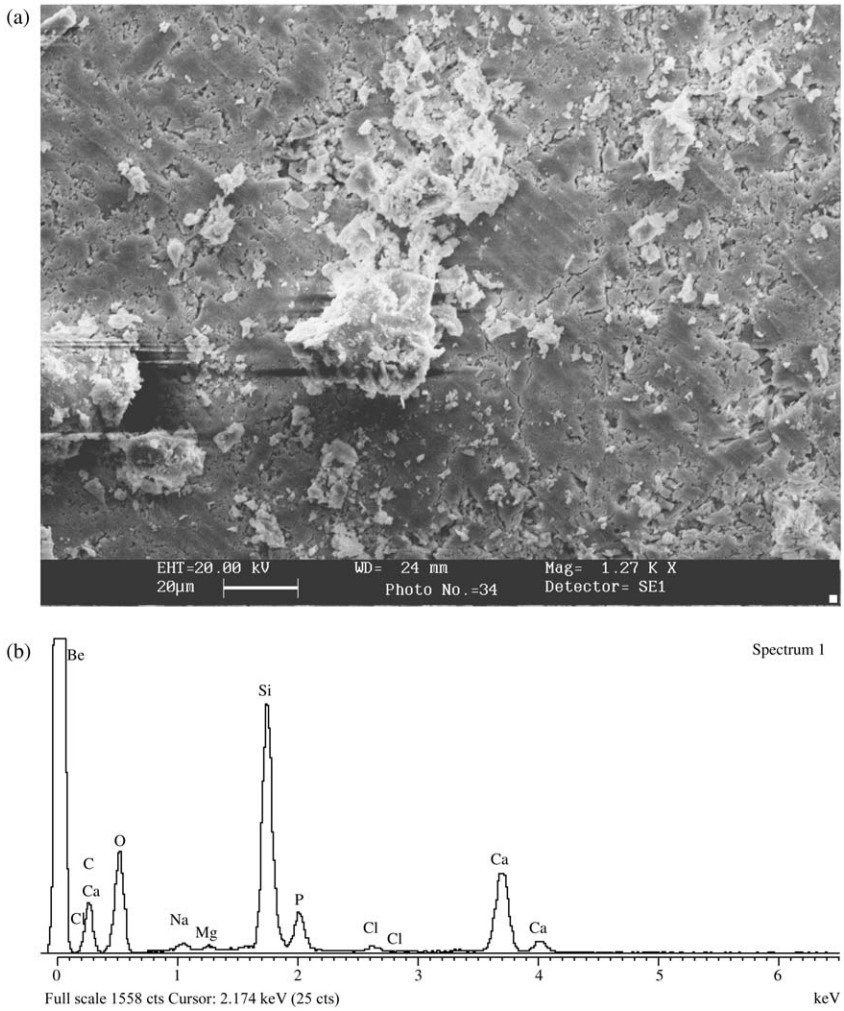

Figure 8 (a) SEM micrograph of the surface of a silver containing sample after 14 days SBF exposed (b) corresponding EDS spectrum.

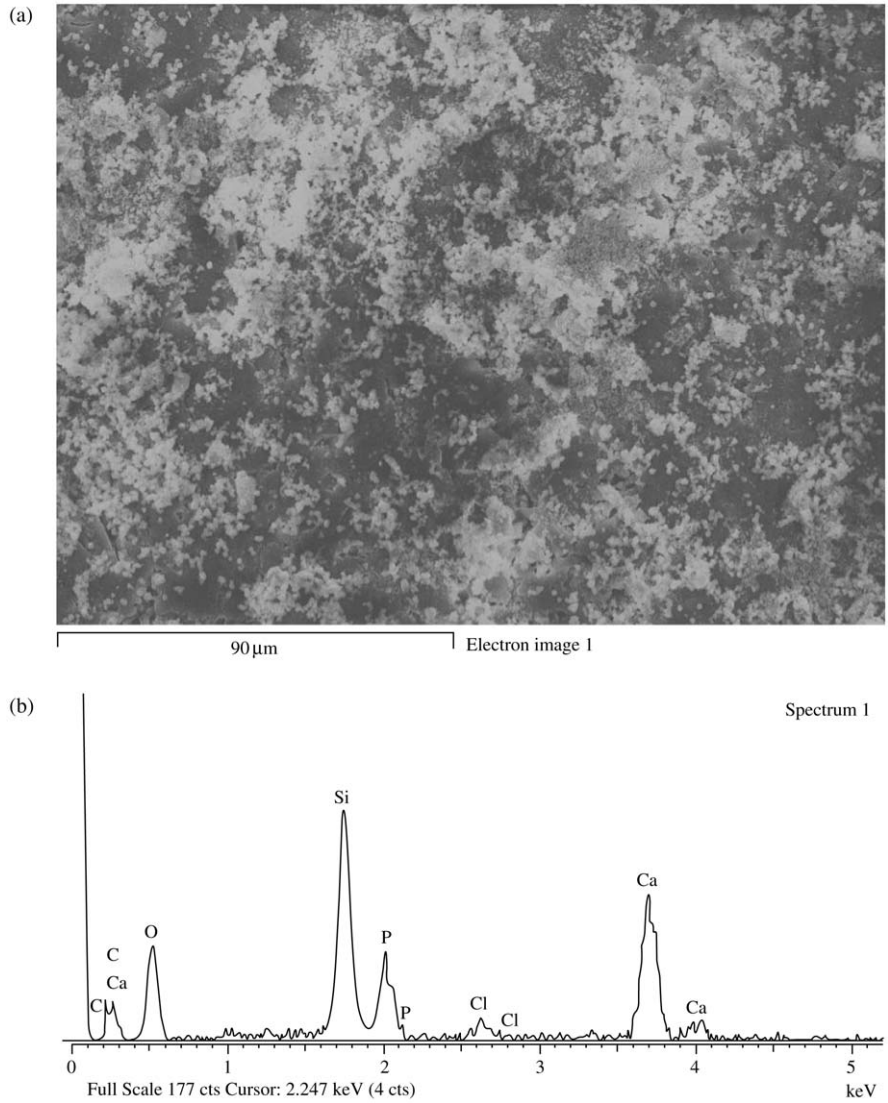

Figure 9 (a) SEM micrograph of the surface of a silver free sample after 14 days SBF exposed (b) corresponding EDS spectrum.

4. Conclusions

Silver containing and silver free silica materials were successfully prepared by sol–gel method. The gel preparation involves hydrolysis and polycondensation tetramethil orthosilicate, sodium ethoxide, calcium nitrate tetrahydrate and silver nitrate using methyl ethyl ketone as solvent. The gel thus prepared is an amorphous solid containing solvent and organic residual that are lost on heating. The necessary temperatures are well below the glass transition temperature of the glass being formed, and therefore, during the heat treatments required for the gel into glass conversion, the gel is kinetically stable to crystallisation. This suggests the possibility of converting the gel glass powders into a monolithic dense glass by sintering or hot pressing technique without devitrification.

The high antibacterial activity of the silver containing gel glass against *E. coli* and *S. mutans* suggests the use of this gel for medical application such as dental restoration. No antibacterial activity was observed in the silver free gel glass of the same composition. Finally the bioactivity of both silver containing and silver free the gel glasses is indicates by FTIR and XRD spectra and SEM micrographs suggest the formation of crystalline HA.

Acknowledgment

This work was supported by POR Campania 2002–2003 (mis. 3.16).

References

1. T. YOSHINARI and M. UCHIDA, *J. Kor. Ceram. Month. February* (1994) 119.
2. J. W. BORETOS, *Adv. Ceram. Mater.* **2** (1987) 15.
3. R. G. T. GEESINK, K. DE GROT and C. P. A. T. KLEIN, *Clin. Orthop.* **225** (1987) 147.
4. Z. SHAOXIAN, Y. ZHIXIONG, L. PING, X. GUANGHONG and C. WANPENG, *Mater. Res. Soc. Symp. Proc.* **292** (1993) 271.
5. T. N. KIM, Q. L. FENG, J. O. KIM, J. WU, H. WANG, G. C. CHEN and F. Z. CUI, *Mater. Sci. Mater. Med.* **9** (1998) 129.
6. S. B. SANT, K. S. GILL and R. E. BURRELL, *Scripta Metall.* **41** (1999) 1333.
7. M. KAWASHITA, S. TSUNEYAMA, F. MIYAJI, T. KOKUBO, H. KOZUKA and K. YAMAMOTO, *Biomaterials* **21** (2000) 393.
8. C. H. Y. LI, Z. WAN, J. WANG, Y. L. WANG, X. Q. JIANG and L. M. HAN, *Carbon* **36** (1997) 61.
9. M. RIVERA-GARZA, M. T. OLGUIN, I. GARCIA-SOSA, D. ALCANTARA and G. RODRIGUEZ-FUENTES, *Microporous and Mesoporous Mater.* **39** (2000) 431.
10. M. BELLANTONE, N. J. COLEMAN and L. L. HENCH, *J. Biomed. Mater. Res.* **51** (2000) 484.
11. T. KOKUBO, *Bol. Soc. Esp. Ceram. Vid.*, Proc. XVI Int. Cong. Glass, Madrid **1**(31-c1) (1992) 119.

12. C. OHTSUKI, T. KOKUBO and T. YAMAMURO, *J. Non-Cryst. Solids* **143** (1992) 84.
13. N. P. BANSAL, *J. Mat. Sci.* **27** (1992) 2992.
14. C. SANCHEZ, J. LIVAGE, M. E. HENRY and F. BABONNEAU, *J. Non-Cryst. Solids* **100** (1988) 65.
15. P. LI and K. DE GROOT, *J. Sol–Gel Sci. Tech.* **2** (1994) 797.
16. D. S. WANG and C. G. PANTANO, *J. Non-Cryst. Solids* **147–148** (1992) 115.
17. I. SIMON and H. O. MCMAHON, *J. Am. Ceram. Soc.* **36** (1953) 160.
18. Y. KIM, A. E. CLARK and L. L. HENCH, **113** (1989) 195.
19. L. L. HENCH, *J. Am. Ceram. Soc.* **74**(7) (1991) 1487.
20. T. N. KIM, Q. L. FENG, J. O. KIM, J. WU, H. WANG, G. C. CHEN and F. Z. CUI, *J. Mat. Sci. Mater. Med.* **9** (1998) 129.

Received 10 June
and accepted 28 October 2003